Correlations in ice-rule ferroelectrics

R. Youngblood and J. D. Axe
Brookhaven National Laboratory, Upton, New York 11973

B. M. McCoy
Institute for Theoretical Physics, State University of New York at Stony Brook, Stony Brook, New York 11794

(Received 26 March 1979)

We discuss the character of long-wavelength polarization fluctuations in model ice-rule ferroelectrics. Because polarization is locally conserved in these systems, polarization correlations are strikingly different in character from those in systems having rotationally invariant correlations. Several aspects of the problem can be discussed quite fruitfully in the language of two-dimensional potential theory. Comparisons are made between predictions of this model family and neutron scattering experiments on a quasi-two-dimensional ice-rule ferroelectric, copper formate tetrahydrate.

I. INTRODUCTION

A recent neutron scattering study[1] of the order-disorder phase transition in copper formate tetrahydrate (CFT) showed that the order-parameter fluctuations in that substance are unusual compared to those accompanying most previously studied phase transformations. In this paper, we will show that those observations are typical of what is to be expected from model two-dimensional (2D) ice-rule systems.[2] In order to put the CFT observations in the proper context, we begin by summarizing some of the relevant features of typical diffuse scattering studies of systems undergoing phase transitions.

In systems governed by short-range forces having finite strength (e.g., Ising systems), the observed diffuse scattering cross section (which gives the spatial Fourier transform of the pair correlations) is approximately a Lorentzian function of the reduced momentum transfer $\vec{q}$.[3] Apart from a possible anisotropy in the correlation length (which can be removed by a coordinate transformation), the pair-correlation function is rotationally invariant, depending only on the distance between sites. The observed scattering cross section has a peak at $\vec{q}=\vec{q}_c$, where $\vec{q}_c$ is the wave vector at which long-range order appears; in principle, when $\vec{q}_c=0$, the magnitude of the scattering at $\vec{q}_c$ is related to a macroscopic susceptibility.

In uniaxial dipolar-coupled systems, the situation is somewhat different. There is a contribution to the correlations which is not rotationally invariant; the differential cross section is singular at $\vec{q}=0$.[4] In the well-known uniaxial ferroelectric potassium diphosphate (KDP), for example, the diffuse scattering can be represented[5] by

$$S(\vec{q})=\{1+\beta[J(\vec{q})+V(\vec{q})]\}^{-1}\ , \tag{1}$$

where $S(\vec{q})$ is the Fourier transform of the displacement-displacement correlation function, β is the inverse temperature, $J(q)$ is the Fourier transform of a short-ranged interaction, $V(\vec{q})\propto(q_l/q)^2$, the small-$|\vec{q}|$ limit of the dipole-dipole potential, and q_l is the longitudinal component of $\vec{q}$ (the component along the uniaxial direction). At small q, $J(\vec{q})$ is rotationally invariant, in the sense described above, but the dipolar term $V(\vec{q})$ destroys the rotational invariance of S. Again, $\lim_{q\to 0}S(\vec{q})$ is related to the macroscopic susceptibility, and the scattering is intense at $q=0$. Note that there is no $\vec{q}$ for which the scattering is predicted to vanish, although the scattering is weaker when $\vec{q}$ is longitudinal than when $\vec{q}$ is transverse. (A more recent discussion of scattering from systems of this type was carried out for the case of $LiTbF_4$.[6])

In CFT, the results are qualitatively different from these two cases. A sample of the neutron diffuse scattering results is shown in Fig. 1, which is a map

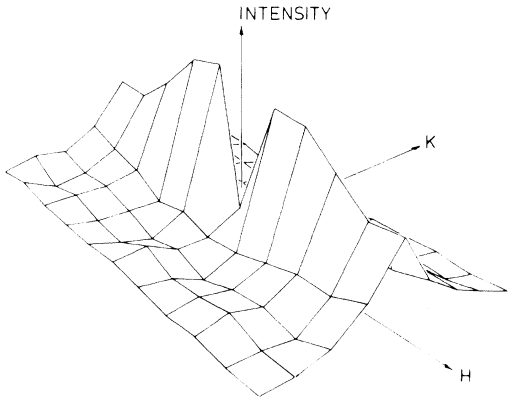

FIG. 1. Shown here some results of a neutron scattering study of finite-wavelength polarization fluctuations in the disordered phase of CFT. (See Ref. 1.)

of

$$I(\vec{Q}) = \langle |F(\vec{Q})|^2 S_{yy}(\vec{q}) \rangle_{av} \ , \tag{2}$$

where $\vec{Q} = \vec{q} + \vec{G}$, $\vec{G}$ is the reciprocal-lattice vector nearest $\vec{Q}$,

$$S_{yy}(\vec{q}) = \sum_{\vec{r}} e^{i\vec{Q}\cdot\vec{r}} \langle P_y(0) P_y(r) \rangle \ ,$$

$|F(Q)|^2$ is a geometrical structure factor which varies slowly with $\vec{Q}$, and the angle brackets with subscript av denote an average over the instrumental resolution function.[7] The subscripts on S indicate that this particular scattering arises from correlations in P_y, the y component of the unit-cell polarization. In general, the cross section includes contributions from other correlations as well; however, making use of the mode analysis given in Ref. 1, one can show that other contributions are suppressed by the structure factor at the point in reciprocal space at which the data in Fig. 1 were taken.

The 2D water layers in CFT lie in crystallographic ab planes; the intralayer reciprocal-lattice coordinates are (h,k). In the ordered phase, the polarization points along $\pm b$, the sign alternating from layer to layer. Thus there are superlattice reflections at half-integral l. The data of Fig. 1, which are centered at such a site, $(h,k,\frac{1}{2})$, were taken at a temperature above the transformation temperature, T_0. At high temperature, the scattering is largely independent of l, showing that the layers are very weakly correlated. Just above T_0 the l dependence of the peaks is more pronounced, demonstrating that a strictly 2D model of the transformation is incomplete. But the qualitative features of the scattering, which are the subject of this paper, are features of ideal isolated 2D layers.

We see in Fig. 1 that the scattering essentially vanishes along the line $h = 0$. Rather than peaking at $\vec{q} = \vec{q}_c$, it peaks at finite transverse $\vec{q}$. As we mentioned earlier, it is typical of uniaxial dipolar-coupled ferroelectrics that the scattering is stronger at transverse $\vec{q}$, but it is not typical for the scattering to vanish in the longitudinal direction. Moreover, $\vec{q}_c$ is, in this case an *anti*ferroelectric superlattice point, at which the dipolar $V(\vec{q})$ is *not* singular; indeed, the existence of the notch was shown in Ref. 1 not to depend on the l coordinate. Therefore, the pattern in Fig. 1 does not arise from a three-dimensional (long-ranged) dipolar coupling. We will see later that this pattern has a basically 2D dipolar character, although its origin is in ice-rule constraints rather than dipolar interactions.

We will show that these results are to be expected in model 2D six-vertex systems. The lattice models we are discussing are the following.[2] Arrows (spins) are assigned to each bond in a square planar array in such a way that two arrows point into and two arrows point away from each vertex (the ice rules). Each of the six allowed vertices in Fig. 2 has a weight,

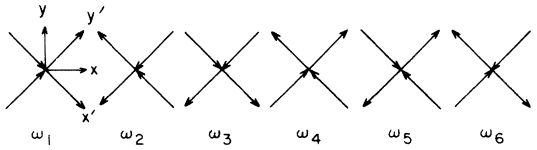

FIG. 2. Six allowed vertices and the associated weights ω_i.

$\omega_i = \exp(-\beta E_i)$. We discuss only the case in which there are no external fields and symmetry requires $\omega_1 = \omega_2$, $\omega_3 = \omega_4$, and $\omega_5 = \omega_6$. The ice, KDP, and F models are special cases. These models are generically termed ice-rule ferroelectric models; they are useful in describing networks of hydrogen bonds, in which protons occupy one of two possible sites along a bond which can be labeled by a spin, $\sigma = \pm 1$. One can imagine associating a physical dipole with each spin; the ice rules insure that the resulting polarization is locally conserved (i.e., "divergenceless" at each lattice site).

A very important characteristic parameter for these models[2] is

$$\Delta = \frac{\omega_1^2 + \omega_3^2 - \omega_5^2}{2\omega_1\omega_3} \ . \tag{3}$$

Prescribing particular energies for the different vertices fixes the interval over which Δ ranges as a function of temperature. If either pair (1,2) or (3,4) is favored, Δ increases from $\frac{1}{2}$ as the temperature decreases from ∞, and ferroelectric order sets in at $\Delta = 1$. Allen[8] has argued that the layers of water molecules in CFT are nearly ideal examples of this behavior. If the pair (5,6) is favored, antiferroelectric long-range order sets in at $\Delta = -1$. The systems we are discussing are thus disordered in the interval $-1 < \Delta < 1$, and the conclusions we draw are valid only for that regime. The other important parameter for our discussion, $\eta = \omega_1/\omega_3$, measures the preference for (1,2) vertices over (3,4) vertices, and thus reflects the intrinsic anisotropy.

It has become increasingly clear that there is a close relation between this problem and several other interesting 2D many-body problems.[9–11] In the discussion of the form of the polarization correlations (Sec. II A), we will see that this problem is governed by standard 2D potential theory.

II. PROPERTIES OF THE CORRELATION FUNCTION AT LARGE R

In this section, we discuss certain properties of the pair correlations at large r. We will draw from three sources of information: Sutherland's[12] exact result for parallel arrow correlations at $\Delta = 0$; the exact results of Fisher and Stephenson[13] for dimer correlations, which can be manipulated to provide complete information about polarization correlations in the

six-vertex model at $\Delta=0$; and studies of the dynamics of the Heisenberg-Ising chain, carried out by Luther and Peschel[14] and Fogedby,[15] which provide some information about the correlations in the six-vertex model at $\Delta \neq 0$. It will be clear by inspection of the six-vertex model results that it is very useful to introduce a "coarse-grained" polarization $\vec{P}(\vec{r})$, which is a local average of the polarization around $\vec{r}$. The leading contribution to the correlations of this quantity are seen at once to be governed by the continuum equation $\vec{\nabla}\cdot\vec{P}=0$. For $\Delta \neq 0$, less information has hitherto been available; however, from the Heisenberg-Ising model results, one can infer the form of the coarse-grained correlations even when $\Delta \neq 0$.

We begin by considering parallel arrow correlations in the six-vertex model, for the case $\eta=1$. Sutherland[12] has shown (see the Appendix) that

$$\langle \sigma_i(0)\sigma_i(\vec{r})\rangle \sim \frac{2}{\pi^2 r^2}\left[(-1)^{x'+y'} - \frac{x'^2-y'^2}{r^2}\right] . \quad (4)$$

where $\sigma_i(\vec{r})$ is the spin pointing along $\pm i$ ($i=x',y'$) at position $\vec{r}=(x',y')$. These coordinates are primed for reasons that will become clear shortly (Fig. 3). One sees in Eq. (4) that there is one contribution to the correlations that oscillates in sign from one lattice site to the next, and another which is smooth. This is also true in the dimer pair correlations (see the Appendix), and in the Heisenberg-Ising correlations (to be discussed shortly). In the CFT problem, these were described[1] as fluctuations of two different modes, one ferroelectric and one antiferroelectric. Our concern here is with long-ranged polarization correlations, or fluctuations in the ferroelectric mode; accordingly, it is useful to introduce the notion of a coarse-grained polarization

$$\vec{P}_{y'}(\vec{r}) = \sigma_{y'}(x',y') + \sigma_{y'}(x'+1,y') .$$

At large $\vec{r}$, the leading contribution to the correlations of the coarse-grained polarization is essentially the smooth contribution, for the values of Δ that we are considering; the rapid oscillations are averaged out. However, two things must be borne in mind. First, the period of the rapid oscillation changes in an applied direct field[12]; in the presence of such a field, the coarse-graining procedure used here would have to be modified. Second, the oscillating contribution decays more slowly than $1/r^2$, for $\Delta<0$ (Ref. 15); it is only the coarse-grained polarization correlations whose leading decay is $1/r^2$. (In considering the coarse-grained polarization, we are essentially taking a step towards a continuum problem which can be discussed in terms of 2D potential theory. But as Δ tends towards -1, the rapidly oscillating contribution becomes increasingly important; ultimately, at $\Delta=-1$, there is a transition to a state of antiferroelectric long-range order, in which the discreteness of the lattice is clearly essential.)

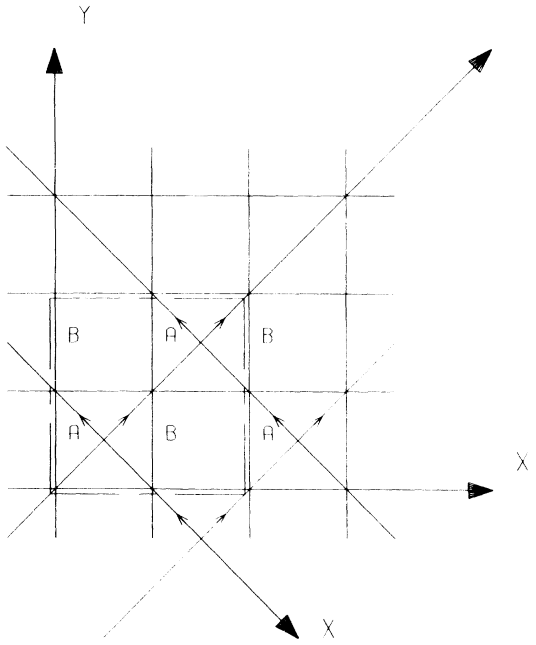

FIG. 3. Here we summarize the connections between the various models discussed in the text. The upright (x,y) coordinate system is that of the dimer problem, whose lattice sites are those of the upright grid. If we designate vertical bonds by A or B in the manner shown, then the y component of the polarization associated with each row is (the number of A dimers minus the number of B dimers) in that row; this polarization is conserved from one row to the next. The primed coordinate system is that of the associated six-vertex problem. As drawn, the arrows correspond to the state of complete polarization along the y axis. In the language of the dimer problem, this is the state having (for example) all A sites occupied by dimers. (See Ref. 8.) The square enclosed by the broken line is the unit cell over which coarse graining is performed. Since the arrows lie along x' or y', the primed coordinates appear to be a natural choice in the six-vertex problem. It is to be emphasized, however, that the ferroelectric order parameter points along x or y. We may think of x' as the Heisenberg-Ising chain axis, and y' as the imaginary time axis. For some purposes, it is useful to think of S^z as pointing along y'.

Another route by which we may evaluate the polarization correlation function uses the correspondence[12,16] between the dimer- and six-vertex models. This route has the advantage of giving the off-diagonal components, $\langle P_i(0)P_j(\vec{r})\rangle$, $(i\neq j)$, as well as the diagonal one considered by Sutherland. It is shown in the Appendix that at $\Delta=0$, and for $\rho=(x^2+\lambda^2y^2)^{1/2}$ large compared to $[\frac{1}{2}(\eta^2+1)]^{1/2}$,

$$\langle P_y(0)P_y(\vec{r})\rangle \sim -A\frac{(x^2-\lambda^2y^2)}{(x^2+\lambda^2y^2)^2} , \quad (5)$$

$$\langle P_y(0)P_x(\vec{r})\rangle \sim A\frac{2\lambda^2xy}{(x^2+\lambda^2y^2)^2} . \quad (6)$$

and

$$\langle P_x(0)P_x(\vec{r})\rangle \sim A\lambda^2\frac{(x^2-\lambda^2y^2)}{(x^2+\lambda^2y^2)^2} \ , \tag{7}$$

where $A=2/\pi^2$, and $\lambda=f_x/f_y$, the ratio of the horizontal and vertical dimer activities. Note that these results are referred to unprimed coordinates. [Of course, these are compatible with Eq. (4), in which $\lambda=\eta=1$.] The unprimed system is special, in that η distinguishes x from y; the ferroelectric order parameter is a polarization which lies along x or y, not x' or y'. Naturally, then, the formulas are simplest in the (x,y) system, if $\eta\neq 1$. (See the Appendix for further discussion.)

All three functions [Eqs. (5)–(7)] are derivable from a single scalar potential. It is instructive to consider this in the light of van Beijeren's[10] correspondence between the six-vertex model and a particular roughening model. If we think of the height h of the interface in that roughening model as a scalar potential $h(x,y)$, we see from van Beijeren's paper that the polarization at six-vertex sites is related to the derivative of $h(\vec{r})$; one has

$$(P_x,P_y)=\left(-\frac{\partial}{\partial y}h(x,y),\frac{\partial}{\partial x}h(x,y)\right)$$

$$=-\vec{\nabla}\times[h(\vec{r})\hat{z}] \ , \tag{8}$$

where $\hat{z}$ is a unit vector in the z direction.

Conservation of polarization ($\vec{\nabla}\cdot\vec{P}=0$) translates into the requirement that $h(x,y)$ be single valued. (Its curl has zero divergence.) Letting $\psi(\vec{R})=\langle h(\vec{r}_0)h(\vec{r})\rangle$, then,

$$\langle P_x(\vec{r}_0)P_x(\vec{r})\rangle=\frac{\partial}{\partial y}\frac{\partial}{\partial y_0}\psi(\vec{R}) \ , \tag{9}$$

$$\langle P_y(\vec{r}_0)P_y(\vec{r})\rangle=\frac{\partial}{\partial x}\frac{\partial}{\partial x_0}\psi(\vec{R}) \ , \tag{10}$$

$$\langle P_y(\vec{r}_0)P_x(\vec{r})\rangle=\frac{-\partial}{\partial y}\frac{\partial}{\partial x_0}\psi(\vec{R}) \ . \tag{11}$$

Bearing in mind that $\psi(\vec{R})=\psi(\vec{r}-\vec{r}_0)$, so that $\partial\psi/\partial x=-\partial\psi/\partial x_0$, etc., one obtains Eqs. (5)–(7) from

$$\psi=-A\ln\rho \ . \tag{12}$$

This has the form of the potential operating between two charges of opposite sign in an anisotropic 2D dielectric medium with $\lambda^2=\epsilon_x/\epsilon_y$.

Conservation of polarization is clearly of paramount importance here, but in itself it is not sufficient to guarantee this result. In particular, the algebraic decay of the correlations is a consequence of the nonexistence of a gap in the eigenvalue spectrum of the transfer matrix, and this state of affairs is easily changed (by application of a staggered field, for example). On the other hand, the conservation law $\vec{\nabla}\cdot\vec{P}=0$ must in any case govern the continuum limit of the coarse-grained polarization correlations. With this in mind, let us consider the case $\Delta\neq 0$.

Studies[14,15] of the 1D Heisenberg-Ising chain, which is governed by the Hamiltonian

$$\mathcal{H}(\Delta)=-\sum_i(S_i^xS_{i+1}^x+S_i^yS_{i+1}^y+\Delta S_i^zS_{i+1}^z) \ , \tag{13}$$

have shown that at large x,

$$\langle S^z(0,0)S^z(x',t)\rangle\sim\frac{-1}{4\pi^2\theta}\frac{(x'^2+v^2t^2)}{(x'^2-v^2t^2)^2}$$

$$+(-1)^{x'}\left(\frac{\xi^2}{(x'^2-v^2t^2)}\right)^{1/2\theta} \ , \tag{14}$$

where[17] $\theta=\frac{1}{2}-(1/\pi)\sin^{-1}\Delta$, and the coordinates are again defined in Fig. 3. Although this result pertains to a different physical model, it is possible to extract information about the six-vertex problem from this. McCoy and Wu[18] showed that the transfer matrix of the six-vertex problem in an applied field commutes with the near-neighbor Heisenberg-Ising Hamiltonian. (Conservation of polarization from one row of a six-vertex lattice to the next is related to conservation of the net magnetization of a 1D chain from one instant of time to the next.) Thus, the eigenvectors of the two operators are the same. Bearing this in mind, consider the correlation between two spins in the same row.

$$g_{y'y'}(x',y'=0)=\langle\lambda_0|\sigma_{y'}(0,0)\sigma_{y'}(x',0)|\lambda_0\rangle \ , \tag{15}$$

where $|\lambda_0\rangle$ is the eigenvector of the largest eigenvalue of the transfer matrix. This quantity depends on the eigenvector $|\lambda_0\rangle$, but not on the eigenvalues; it can therefore be identified with $\langle S^z(0,0)S^z(x',0)\rangle$ given above. Of course, the situation is different for $t'\neq 0$. Note in this connection that the six-vertex problem under discussion has two nontrivial parameters, η and Δ; the above Heisenberg-Ising Hamiltonian has only one. It can also be seen in Fig. 3 that the two problems have incompatible mirror planes; we expect

$$\langle S^z(0,0)S^z(x',t)\rangle=\langle S^z(0,0)S^z(-x',t)\rangle \ ,$$

but not

$$\langle\sigma_{y'}(0,0)\sigma_{y'}(x',y')\rangle=\langle\sigma_{y'}(0,0)\sigma_{y'}(-x',y')\rangle \ ,$$

since the x and y axes are distinguished by the anisotropy η. The similarity between Eqs. (14) and (5) is almost misleading; the two appear to be nearly the same for $\eta=1$, $\Delta=0$.

We may summarize the situation as follows. Even though we cannot make immediate use of Eq. (14) for $t\neq 0$, the form of $\langle P_i(0,0)P_j(x,y)\rangle$ is clear. Equation (14) prescribes the normal derivative of ψ everywhere on the edge of the half-plane defined by

the x' axis. Equations (9)–(12) continue to govern the correlations for $\Delta \neq 0$, with A and λ now depending on Δ. On comparing Eqs. (5) and (14), we arrive at the result that

$$A(\Delta) = (\pi^2\theta)^{-1} \quad . \tag{16}$$

When $\lambda(\eta, \Delta \neq 0)$ is known, information concerning the asymptotic behavior of the polarization correlations will be complete. Further arguments concerning $\lambda(\eta, \Delta)$ will be presented elsewhere.

III. PROPERTIES OF THE SCATTERING CROSS SECTION

The intensity of diffuse neutron or x-ray scattering probing the small $|\vec{q}|$ fluctuations in P_y is proportional to

$$S_{yy}(\vec{q}) = \sum_r e^{i\vec{q}\cdot\vec{r}} \langle P_y(0) P_y(\vec{r}) \rangle \tag{17}$$

Transforming Eq. (5), we find

$$S_{yy}(\vec{q}) = 2\pi A \frac{\lambda h^2}{\lambda^2 h^2 + k^2} = \frac{2\pi A \lambda}{\lambda^2 + (k/h)^2} \tag{18}$$

at small $|\vec{q}|$. This function is plotted in Fig. 4. It is particular in that it depends only on the ratio (h/k), not on the magnitude $|\vec{q}|$. (By studying diagrammatic expansions of the correlation functions, Villain[19] arrived at a similar conclusion for the case of three-dimensional ice.) This has to do with the fact that the sum over $\vec{r}$ of $g(\vec{r})$ is conditionally convergent. A discussion of this point will be presented elsewhere.

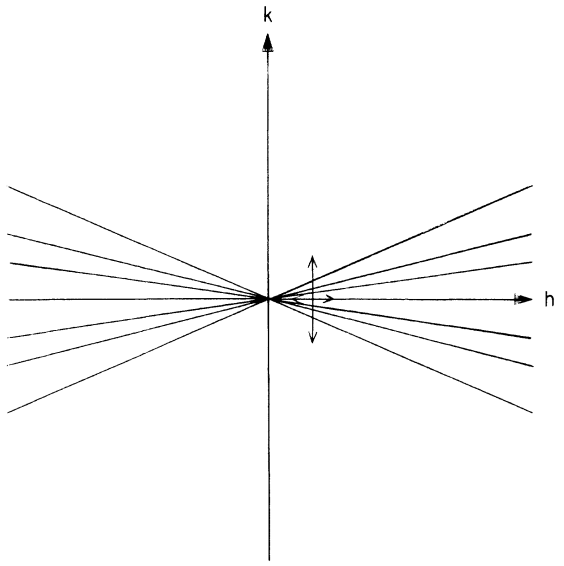

FIG. 4. This is a schematic contour plot of $S_{yy}(h,k)$. All the contours meet at $\vec{q}=0$. The arrows indicate widths of an instrumental resolution function. When the resolution function is centered at $q=0$, the intensity [Eq. (18)] is small; when it is centered at large h, with $k=0$, maximum intensity is picked up.

Recall [Eq. (3)] that in a scattering experiment, one measures an average of the differential cross section over an instrumental resolution function. For example, if the resolution function is Gaussian—frequently a good approximation[7]—then

$$I(h,k) \propto \frac{1}{\sigma_h \sigma_k} \int\int \exp\frac{-\delta_h^2}{2\sigma_h^2} \times \exp\frac{-\delta_k^2}{2\sigma_k^2} S(h+\delta_h, k+\delta_k) \times d\delta_h\, d\delta_k$$

$$= \sum_r \tilde{g}(r) e^{i(hx+ky)} \quad . \tag{19}$$

where

$$\tilde{g}(\vec{r}) = g(\vec{r}) \exp(-\tfrac{1}{2}\sigma_h^2 x^2) \exp(-\tfrac{1}{2}\sigma_k^2 y^2) \quad .$$

σ_h, σ_k are resolution widths along h,k, and δ_h, δ_k are deviations from the nominal $\vec{q}$. From this, is can be seen that the shape of Eq. (18) cannot be directly observed in a scattering experiment. The peculiar nonanalyticity is a consequence of the range of $g(\vec{r})$; as seen with realistic resolution, however, $\tilde{g}(r)$ decays as $r^{-2}\exp(-r^2)$ rather than as r^{-2}. To put it another way, $I(h,k)$ is, of necessity, a smooth, well-defined function of (h,k) while $S(h,k)$ is not.

To understand what is seen in a scattering experiment, it is useful to consider a particular limiting case of Eq. (19). Let σ_h be very small, and consider $I(h,k)$ along the line $k=0$. According to Eq. (18), $S(h,k)$ is a Lorentzian function of k, whose width is proportional to $|h|$. At sufficiently small $|h|$, then, the integral over k essentially sums $S(h,k)$, because the resolution function is effectively constant compared to $S(h,k)$. Therefore, at small $|h|$, we can write

$$I(h,k=0) \propto \int_{-\sigma_k}^{\sigma_k} g_{yy}(h,\delta_k)\, d\delta_k = 4\pi A h \tan^{-1}\left(\frac{\sigma_k}{h\lambda}\right) \quad . \tag{20}$$

The intensity is predicted to go to zero as $|h|$. In fact, by integrating (h,k) over k, we have simply recovered the one-dimensional Fourier transform of $g_{yy}(x,y=0)$, since

$$\int dk\, S(h,k) \propto \sum_{x,y} g(r) e^{ihx} \int dk\, e^{iky}$$

$$\propto \sum_{x,y} g(r) e^{ihx} \delta(y) \quad . \tag{21}$$

The form of Eq. (20), then, is the experimental sig-

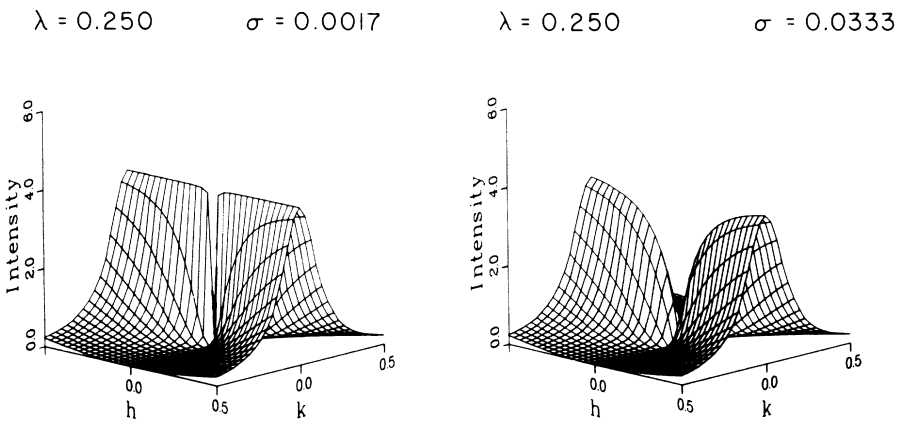

FIG. 5. Plots of S_{yy} averaged as in Eq. (19) for two different values of σ_k, with $\sigma_h = 0$.

nature of the $1/r^2$ decay of $g(r)$. Of course, in a real experiment, σ_h does not approach zero, so Eq. (20) could not be taken literally even in an ideal ice-rule system. But in Fig. 5 of Ref. 1, we show that the observed intensity does resemble the prediction of Eq. (20), and these data were taken with a relatively narrow σ_h.

The effect of resolution is illustrated in Fig. 5, in which we show plots of Eq. (19) for two different values of σ_k with $\sigma_h = 0$. $S_{yy}(h,k)$ is assumed to be given by its small-q form, with A held constant [see Eq. (22)]. The larger value of σ_k corresponds to that used in the experiments. In Fig. 6 we plot Eq. (23) for two different values of λ. Note that the overall shape is governed by the relation between σ_k and λ. Finally, in Fig. 7 we include the geometrical structure $|F(Q)|^2$ appropriate to CFT [see Eq. (2)]. The qualitative features of Fig. 1 are clearly present in Fig. 7. In making this comparison, one should remember two things: we have used the small-q form of $S(h,k)$; and the values of λ were chosen arbitrarily.

Since any real system has ice-rule violations, one has to clarify how the ideal ice-rule case can meaningfully be compared to experiment. The conditional convergence of $\sum_{\vec{r}} g(\vec{r})$ is due, in part, to the ice rules; for example, the eight-vertex model, which we can think of as a six-vertex model with special defects, has exponentially decaying correlations[17] except as T_c, so there is no problem is summing them. What does one expect to see in a scattering experiment? Curiously, in changing algebraic decay to exponential decay, defects partially mimic the effects of finite resolution, which changes the apparent rate of decay of $g(r)$ [Eq. (19)]. Defects will change the correlations primarily at large r; the cross section therefore changes primarily at q less than the inverse of the characteristic defect separation, that is, only at small q. If the spectrometer's q resolution is much larger than this characteristic inverse length, defects will make little difference in the observations. This appears to be the case in the observations made so far in CFT.

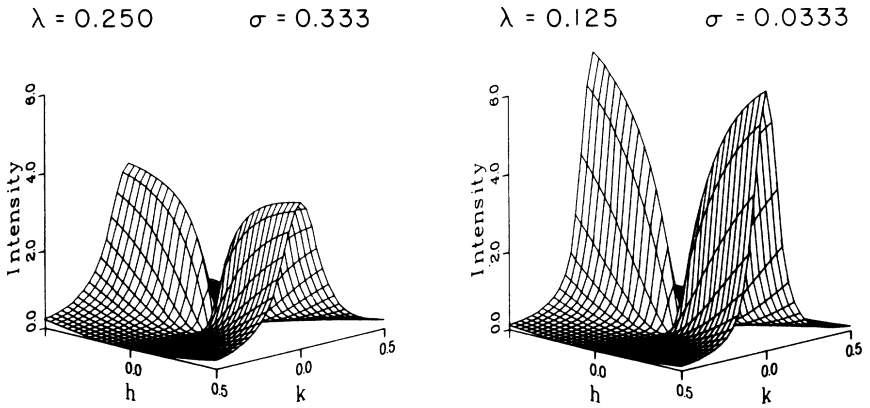

FIG. 6. S_{yy} is averaged with a σ_k corresponding to that used in the experiments for two different values of λ.

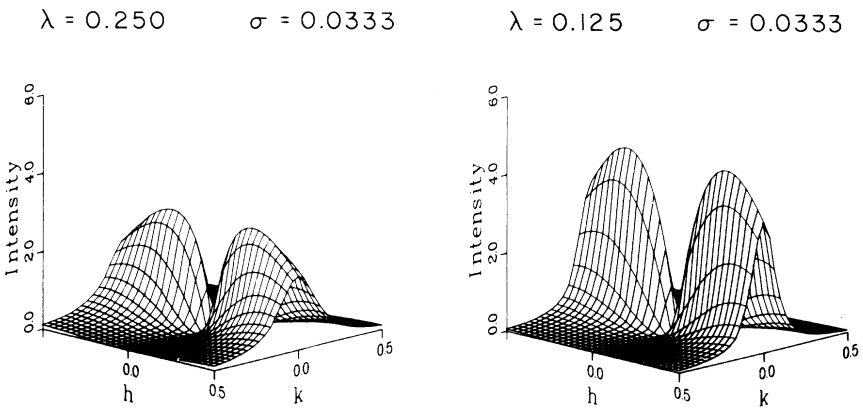

FIG. 7. Here we include the geometrical structure factor $|F(Q)|^2$ [Eq. (2)] appropriate to the CFT problem; the intensity is plotted for two different values of λ over the entire Brillouin zone.

IV. SUMMARY

Typically, the critical fluctuations observed in a scattering experiment are approximately of Lorentzian form, $S(\vec{q}) \sim (\kappa^2+q^2)^{-1}$. This implies that the correlation function $C(R)$ behaves as a *monopolar* field; i.e., $C(R) \sim R^{-1}e^{-\kappa R}$ for $d=3$, $C(R) \sim K_0(\kappa R)$ for $d=2$, etc.[20]; these correlations are rotationally invariant. By contrast, the asymptotic behavior of the polarization correlations in 2D ice-rule systems is the potential between a pair of 2D dipoles, $\underline{C}(\vec{R}) \sim \vec{\nabla}_r \vec{\nabla}_{r'} \ln\rho$. These correlations are *not* rotationally invariant. Moreover, because of the range of this correlation function, the differential scattering cross section is singular in the small-q limit. This is ultimately not observable in a scattering experiment. First, in a real system, ice-rule violations formally remove the singularity. Second, in a real experiment, finite resolution would wash out the singularity if it were present.

Scattering measurements nonetheless retain considerable power, as the measurements on CFT have demonstrated. It is certainly possible to assess the relative importance of monopolar and dipolar contributions. (The former are negligibly small in CFT.) Moreover, it is possible to measure $S(\vec{q})$ at small but finite $|\vec{q}|$. In addition to the (thus far qualitative) information that these data convey directly, we can also use them to evaluate various useful integrals of $S(\vec{q})$. The features which are measurable in scattering experiments are likely to be resistant to defects. Indeed, although ideal (defect-free) ice-rule systems presumably do not exist, effects of the kind discussed here are to be expected in other (in particular $D=3$) systems. It is likely that CFT is unusual only in providing a clearcut $D=2$ example.

ACKNOWLEDGMENTS

Part of this work was performed while two of us (R.Y.and J.D.A.) were in residence at Risø National Laboratory. We are grateful for the warm hospitality we found there. Two of us (R.Y. and J.D.A.) have been influenced by stimulating discussions on this subject with a number of people, including V. J. Emery, J. F. Nagle, and J. Villain. The work at Brookhaven was supported by the Division of Basic Energy Sciences, DOE, under Contract No. DE-AC02-76CH00016. The work at Stony Brook was supported by the NSF under Grant No. DMR-7707863A01.

APPENDIX

In this Appendix, we outline the derivation of the asymptotic behavior of pair correlations for the dimer- and six-vertex models. We begin by extending the analysis of dimer correlations performed by Fisher and Stephenson (FS).[13] We use these results to discuss the polarization correlations in CFT, making use of a correspondence introduced by Allen.[8] The necessary connections between the dimer- and six-vertex models were established by Baxter.[16]

In the dimer model, a square array of N lattice points are covered by $\frac{1}{2}N$ "dimers," a dimer being a linked pair of nearest-neighbor lattice sites. Only one dimer can be associated with any lattice site. Anisotropy is introduced through different activities, $f_{x,y} \equiv \exp(-u_{x,y}/kT)$ for dimers lying along x and y axes (referred to as horizontal and vertical dimers, respectively).

FS define the correlation function for two dimers

separated by s horizontal bonds and t vertical bonds in terms of a product of Green's functions, (s,t). For example, for two horizontal dimers

$$C_{xx}(s,t)=f_x^2[(s-1,t)(s+1,t)-(s,t)^2] \quad . \tag{A1}$$

The remaining correlation functions are similarly defined. (s,t) is defined in terms of a double integral

$$(s,t)=\frac{f_x}{2\pi^2}\int_0^\pi d\alpha\, g(\alpha,s)\int_0^\pi d\beta\,\frac{h(\beta,t)}{\Delta(\alpha,\beta)} \tag{A2}$$

for odd s and even t. $(s,t)=0$ for s,t both even or both odd, and for even s and odd t, (s,t) is obtained from Eq. (A2) by a permutation of the arguments of g and h. In Eq. (A2)

$$g(\alpha,s)=\cos\tfrac{1}{2}(s+1)\alpha-\cos\tfrac{1}{2}(s-1)\alpha$$
$$=-2\sin\tfrac{1}{2}\alpha\sin\tfrac{1}{2}s\alpha \quad ,$$
$$h(\beta,t)=\cos\tfrac{1}{2}t\beta \quad ,$$

and

$$\Delta(\alpha,\beta)=f_x^2(1-\cos\alpha)+f_y^2(1-\cos\beta) \quad .$$

FS evaluate (s,t) exactly for $|s|+|t|\leq 11$, and they discuss the asymptotic behavior of $(s,t=0)$ and $(s=0,t)$. Using a different method, we extend the evaluation to general s,t in the asymptotic limit.

The integral on β may be performed exactly:

$$I(\alpha,t)=\int_0^\pi d\beta\,\frac{h(\beta,t)}{\Delta(\alpha,\beta)}$$
$$=\frac{\pi}{B(1-a^2)^{1/2}}\left[\frac{(1-a^2)^{1/2}-1}{a}\right]^{t/2} \tag{A3}$$

and

$$I(\alpha)\approx\frac{\pi}{\alpha f_x f_y}e^{-\lambda t|\alpha|/2}$$

for large t. Here

$$B=f_x^2(1-\cos\alpha)+f_y^2 \quad ,$$
$$a=-f_y^2/[f_x^2(1-\cos\alpha)+f_y^2] \quad ,$$

and $\lambda=f_x/f_y$. Since $I(\alpha)$ is sharply peaked about $\alpha=0$ for large t, the integral in Eq. (A2) on α can now be performed with the substitution of Eq. (A3) to obtain the asymptotic behavior of (s,t) by Laplace's method. The result, in the limit of large s, is

$$(s,t)\sim\begin{cases}\dfrac{-1}{\pi}\dfrac{f_y s}{(f_y s)^2+(f_x t)^2} & (s \text{ odd}, t \text{ even}) \quad , \quad \text{(A4)}\\[2ex] \dfrac{i}{\pi}\dfrac{f_x t}{(f_y s)^2+(f_x t)^2} & (s \text{ even}, t \text{ odd}) \quad . \quad \text{(A5)}\end{cases}$$

Given (s,t), the dimer correlation functions are readily evaluated from expressions given in FS.

It remains to make the correspondence between dimer and polarization fluctuations. As discussed in Refs. 1 and 8, the correspondence is such that a 2×2 cell on the dimer lattice represents a single unit cell in a CFT layer. The state of uniform $x(y)$-axis polarization corresponds to a configuration involving only horizontal (vertical) dimers which are staggered in adjacent rows and columns. If we introduce the operator $\nu_\alpha(s,t)=0$ or 1, which measures the dimer occupation of a given bond on the dimer lattice, then it follows that the local coarse-grained polarization operator on the CFT lattice consistent with that defined in the text for the six-vertex model is

$$P_\alpha(\tfrac{1}{2}s,\tfrac{1}{2}t)=\tfrac{1}{2}[\nu_\alpha(s,t)-\nu_\alpha(s,t+1)$$
$$-\nu_\alpha(s+1,t)+\nu_\alpha(s+1,t+1)] \tag{A6}$$

where we take (s,t) to be even. It is then a simple matter to show that

$$\langle P_\alpha(\tfrac{1}{2}s,\tfrac{1}{2}t)P_\beta(0,0)\rangle$$
$$=\sum_{m,n=0,1}(-1)^{m+n}C_{\alpha\beta}(s+m,t+n) \quad , \tag{A7}$$

for $s,t\gg 1$. The explicit results are

$$\langle P_x(\tfrac{1}{2}s,\tfrac{1}{2}t)P_x(0)\rangle\sim 2\frac{f_x^2}{\pi^2}\frac{p^2-q^2}{(p^2+q^2)^2} \quad , \tag{A8}$$

$$\langle P_x(\tfrac{1}{2}s,\tfrac{1}{2}t)P_y(0)\rangle\sim 2\frac{f_x f_y}{\pi^2}\frac{2pq}{(p^2+q^2)^2} \quad , \tag{A9}$$

$$\langle P_y(\tfrac{1}{2}s,\tfrac{1}{2}t)P_y(0)\rangle\sim -2\frac{f_y^2}{\pi^2}\frac{(p^2-q^2)}{(p^2+q^2)^2} \quad , \tag{A10}$$

where $p=f_y s$ and $q=f_x t$.

Now we turn to the related problem of pair correlations in the six-vertex model. For $\Delta=0$, the problem reduces to a free fermion model, and Sutherland[12] was able to calculate the diagonal (i.e., vertical arrow-vertical arrow) correlations $g_{y'y'}(\vec{r})$. He presented explicit expressions for the asymptotic behavior only in the isotropic ($\eta=1$) limit. We extend these results into the $\eta\neq 1$ regime, and compare the results with those just derived for the dimer model.

Sutherland finds that, in the absence of long-range order and with no external fields, the diagonal pair correlations are given by

$$g_{y'y'}(x',y')=(1/\pi^2)I_1(x',y')I_2(x',y') \quad , \tag{A11}$$

where

$$I_1=\int_{\pi/2}^{3\pi/2}[f(ik)]^{y'}e^{ix'k}dk \quad , \tag{A12}$$

$$I_2=\int_{-\pi/2}^{\pi/2}[f(ik)]^{-y'}e^{-ix'k}dk \quad , \tag{A13}$$

and $f(ik)=(\eta+e^{ik})/(\eta e^{ik}-1)$. Here x' and y'

measure the number of intervening bonds along the x' and y' directions, respectively (see Fig. 3). Making use of the relation $f(i(k+\pi)) = -[f(-ik)]^{-1}$, we find that $I_2 = (-1)^{x'+y'} I_1^*$ and thus

$$g_{y'y'}(x',y') = [(-1)^{x'+y'}/\pi^2]|I_1(x',y')|^2 \quad . \tag{A14}$$

In order to evaluate $I_1(x',y')$ asymptotically, we write it as a contour integral in the complex plane with the intention of using a method of steepest descents.

$$I_1(x',y') = \int_c [f(z)]^{y'} z^{x'} \frac{dz}{iz}$$

$$= \int_c \frac{dz}{iz} \exp[w(z)] \quad . \tag{A15}$$

If we write $z = re^{i\Phi}$ and $f(z) = R(z)e^{i\Phi(z)}$ then

$$w(z) = (y' \ln R + x' \ln r) + i(y'\Phi + x'\phi)$$

and the contour is taken clockwise on a unit semicircle from $-i$ to $+i$. Consideration of the integrand reveals that the important contributions to I_1 come not from saddle points but from the end points of the integral, where $\mathrm{Re}[w(z=\pm i)] = 1$. The integration is performed by deforming the contours in the vicinity of the end points to coincide with paths of steepest descent for $\mathrm{Re}[w(z)]$. If, for example, such a path around $z = i$ is specified by $z = i + se^{i\Phi}$, it is found that the contribution to the integral can be approximated as

$$I_+ \sim -(i)^{x'+y'} e^{i\theta} \int e^{-Ds} ds = -(i)^{x'+y'} e^{i\theta}/D \quad . \tag{A16}$$

with

$$\tan\theta = 2\eta y'[(\eta^2+1)x' - 2\eta y']^{-1} \quad . \tag{A17}$$

$$D^2 = x'^2 - 2\beta x'y' + y'^2$$

$$= [2/(\eta^2+1)](x^2 + \lambda^2 y^2)$$

$$\equiv [2/(\eta^2+1)]\rho^2 \quad . \tag{A18}$$

$$\beta = (\eta^2-1)/(\eta^2+1) \quad . \tag{A19}$$

[Note that it is D, not $r = (x'^2+y'^2)^{1/2}$, which plays the role of the large parameter in the asymptotic expansion. This means that the asymptotic expansion is not valid for any combination of parameters for which D is not much larger than unity. This occurs, for instance, as $\eta \to \infty$, even for arbitrarily large $x' = y'$. Analogous comments pertain concerning the large parameter in the asymptotic expansion of the dimer correlations.] The contribution to I_1 from the $z = -i$ end point is of the form $I_- = I_+^*$; on evaluation, one obtains the final result for $g_{y'y'}(x',y')$,

$$\langle \sigma_{y'}(0)\sigma_{y'}(\vec{r}) \rangle$$

$$\sim -\frac{2}{\pi^2 D^2}\left[(-1)^{x'+y'} + \frac{(1-2\beta^2)y'^2 + 2\beta x'y' - x'^2}{D^2}\right] \tag{A20}$$

This reduces to Eq. (4) for the isotropic case, $\eta = 1$, and the coarse-grained part of the expression is identical to that obtained from Eqs. (5)–(7) by a transformation from the (x,y) to (x',y') coordinate system.

[1] R. Youngblood and J. D. Axe, Phys. Rev. B 17, 3639 (1978).

[2] For a review, see the article by E. H. Lieb and F. Y. Wu, in *Phase Transitions and Critical Phenomena*, edited by C. Domb and M. S. Green (Academic, New York, 1977).

[3] C. A. Tracy and B. M. McCoy, Phys. Rev. B 12, 368 (1975).

[4] M. A. Krivoglaz, Sov. Phys. Solid State 5, 2526 (1964).

[5] G. L. Paul, W. Cochran, W. J. L. Buyers, and R. A. Cowley, Phys. Rev. B 2, 4603 (1970).

[6] J. Als-Nielsen, Phys. Rev. Lett. 37, 1161 (1976).

[7] M. J. Cooper and R. Nathans, Acta Crystallogr. 23, 357 (1967).

[8] G. R. Allen, J. Chem. Phys. 60, 3299 (1974).

[9] S. T. Chui and J. D. Weeks, Phys. Rev. B 14, 4978 (1976).

[10] H. van Beijeren, Phys. Rev. Lett. 38, 993 (1977).

[11] J. V. Jose, L. P. Kadanoff, S. Kirkpatrick, and D. R. Nelson, Phys. Rev. B 16, 1217 (1977).

[12] B. Sutherland, Phys. Lett. A 26, 532 (1968).

[13] M. E. Fisher and J. Stephenson, Phys. Rev. 132, 1411 (1963).

[14] A. Luther and I. Peschel, Phys. Rev. B 12, 3908 (1975).

[15] H. C. Fogedby, J. Phys. C 11, 4767 (1978).

[16] R. J. Baxter, Ann. Phys. (N.Y.) 70, 193 (1972).

[17] J. D. Johnson, S. Krinsky, and B. M. McCoy, Phys. Rev. A 8, 2526 (1973).

[18] B. M. McCoy and T. T. Wu, Nuovo Cimento B 56, 311 (1968).

[19] J. Villain, Solid State Commun. 10, 967 (1972).

[20] M. E. Fisher, Physica (Utrecht) 28, 172 (1962).